HNPS Advances in Nuclear Physics

The expansion of TRIAC to TRIACII code for track measurements from SSNT detectors

D. L. Patiris, K. Blekas, K. G. Ioannides

The expansion of TRIAC to TRIACII code for track measurements from SSNT detectors

D. L. Patiris[a], K. Blekas[b] and K. G. Ioannides[a].

[a]Nuclear Physics Laboratory, Department of Physics, The University of Ioannina ,
451 10 Ioannina, Greece.

[b]Department of Computer Science, The University of Ioannina ,451 10 Ioannina, Greece.

The expansion of TRIAC to TRIACII code will be described. Both codes have been developed for recognition and parameters measurements of particles' tracks from images of Solid State Nuclear Track Detectors. While the first program considers the tracks as circles, TRIACII code, using image analysis tools, counts the number of tracks and depending on the current working mode classifies them according to their radii (Mode I- circular tracks) or their axis (Mode II- elliptical tracks), their mean intensity value (brightness) and their orientation. Hough transform techniques are used for the estimation of tracks' number and their parameters which are able to give results even for overlapping tracks. The new program has been used for radon's progeny behavior and alpha particles' energy discrimination.

1. Introduction

The naturally occurring radon gas and its decay products are responsible for approximately half of the total radiation dose received by the public.[1] Solid State Nuclear Tracks Detectors (SSNTD) are polymer dielectric materials, widely used in radon research. Charged particles from protons upwards but not -particles nor photons lead to intensive ionization when they pass through these detectors. Along the path of the particle a damaged region is created, usually named latent track, with diameters only some tens of nm. A chemical etching procedure with a suitable etchant (NaOH or KOH) etches the detector's surface but with a faster rate along the damaged regions. As a result the latent tracks become permanent and can be sufficiently enlarged in order to be visible under an optical microscope. The shapes of the tracks are generally elliptical. For a standard chemical etching procedure the size, the brightness and the orientation of the track's ellipse are strongly dependent on the particles' charge, energy and incident angle.[2] The computer code described in this paper has been used by the authors for radon measurements and for the differentiation of -particles' energies.[3] The code uses as input files a number of images in .jpg format recorded from SSNTD's surface. As output the user is provided with files in which the number of the recognized tracks is presented as well as tracks' parameters, such as the mean intensity values (brightness) and the orientation.

2. Computer code

2.1. General information

The program TRIAC II is written in the high level language MatLab, which is accompanied by a variety of tools for special applications. It runs in two different modes followed by the corresponding calibration actions. The first mode is dedicated to the estimation of the number of the tracks from a SSNTD's surface image. The accurate measurement of the number of tracks is important for reliable radiation dose estimations. Usually, a number of images is required, containing as many tracks as possible for improved statistics. To include a large number of tracks in an image, lenses of low magnification are used. As a result, most tracks are resolved as circles. For this reason the program counts the tracks as circles, when is functioning in the first mode. On the other hand, in the second mode the user is provided with the parameters of the recognized tracks, which in general have elliptical shapes. The major and minor axes (in pixels), the mean value of brightness and the orientation (in degrees) of the tracks are output in files. The results are more accurate if a lens of higher magnification is used. Also, in the calibration modes a group of images are provided on screen. This group contains the initial and a number of analyzed images produced after important program steps. The aim of the calibration modes is to help the user to set the input program parameters, which fit better to his/her criteria. Finally, TRIAC II is supplied with a GUI which facilitates the entry of input parameters and the choice of actions.

2.2. Image segmentation

An image from SSNTD's surface is for MatLab a two-dimensional matrix of size equal to the image's digital resolution. The first step to the analysis is the image segmentation task that groups the image pixels together and separates the objects (useful information) from the background. A variety of methods have been proposed for image segmentation, such as edge-based or region-based methods.[4] Amongst them, histogram-based clustering methods have been proved very efficient, since they basically correspond to clustering approaches. A well known clustering method is the K-means algorithm [5], which tries to appropriately adjust the K cluster centers in order to minimize the distance from each data point to its nearest center.

Due to its local search, a known drawback of the algorithm is the initialization of their parameters (centers). This is accomplished by uniformly selecting a small subset of the pixel intensities (e.g. 10) and executing the algorithm several times. The optimum solution found is then used for initializing the cluster centers. The number of these cluster centers K is given by the user. As has been observed, the input images, apart from the background (light pixels) and the track regions (dark pixels), contain a middle level(s) of brightness pixel regions (grey). This is happened due to system imperfections during the generation process. Therefore, a value of K = 3 or 4 is used for the number of clusters during the clustering procedure, in order to best distinguish the useful information (track objects) from the rest parts of the images. At the end of the segmentation process, every pixel is labeled to a discrete value in the range of [1, K] based on the cluster it belongs (minimum distance from the cluster centers). Since we are interested in the track objects, a binary image is finally produced by setting to one (1) only the darker pixels and leaving the rest to zero (0).

Before the image segmentation during only the second mode of TRIAC II a brightness normalization procedure of the initial image is performed. This step has the aim to reduce the influence of apparatus characteristics or imperfections to the measurements of pixel intensities. In some cases photos containing particles' tracks may have not uniform light background. In addition apparatus's imperfections have as a result the detector's photo to contain "objects" which are not real tracks. An example is shown in the Figure 1(a). The center of the image is brighter and if a track was there the mean brightness

(a) Initial track image   (b) BrightNormal   (c) Normalized image
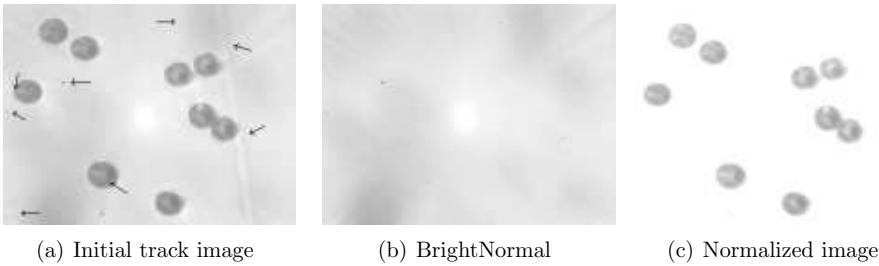
Figure 1. An example of the brightness normalization procedure.

value would be overestimated. Also, there are some "track-like" objects which are not tracks. These phenomena can increase the number of observed tracks and can cause the accuracy of brightness measurements. The Brightness normalization step obliterates such problems. A user in addition with the detector's photos has to include another "special" one. For this photo, it is very important to keep exactly the same apparatus adjustments (ie magnification, focusing) with which the tracks' photos were recorded but without the detector. Grey scale pixel values of this photo, which must be named "BrightNormal.jpg" [Figure 1(b)] and its aim is to "be subtracted" from all the tracks' photos. An example of the final "Normalized" image is shown in the Figure 1(c).

2.3. Image Morphology

TRIAC II performs two types of morphological operations to the binary image which is produced from the segmentation task. The first uses an input parameter named morphological threshold provided by the user, aims to remove small objects whose number of interconnected pixels is less than the user set threshold value. Depending on the size and characteristics of the image, this value should be adjusted, the higher the threshold value is set then larger objects will be removed. Furthermore, a statistical operation follows. After removing small objects, the program performs an initial estimation of all objects sizes and their average size together with the associated standard deviation. Then, any object with size greater than the mean value plus n-times the standard deviation is removed. This last input value (n) named statistical check value is related to the procedure described above and which aims to remove imperfections of the detectors' surface or other oversized objects that are not tracks. Setting this value low we allow more objects to be

removed since their size exceeds the average size. The morphological threshold value and the statistical check value may be determined using the Calibration Modes.

2.4. Tracks Detection

The next step of our analysis is the determination of the number, as well as the geometric features of the tracks in the isolated objects of the resulting binary image. These objects may contain one or more overlapping tracks. In order to separate them, we followed the next strategy: In each object, we initially perform the Canny edge detection algorithm [6] to find object boundaries in the image. The known Hough transform [7],[8] approach is then applied to identify the geometric structure of the tracks. In the first mode as it was already mentioned, the tracks are considered circular so we apply the circular Hough transform. In this way, we extract the length of the diameter (in pixels) and the mean intensity value of each detected circular track. In the second mode a more complicated procedure is followed dealing with the general case of the elliptic shape of tracks. Here, we apply the Hough transform approach for ellipses [8] and the output includes four features: the major axis, the minor axis, the orientation of the ellipse, and the mean intensity value of the surrounding pixels. In either case, we build an appropriate Hough space of dimensions equal to the parameters of the assumed geometric shape (circle or ellipse), where its strongest peaks correspond to the number of the overlapping tracks in the object. Once the strongest peak is found, the value of the accumulator function in the surrounding pixels becomes zero to repeatedly avoid detecting the same geometric shape. An example of the whole procedure is presented in Figures 2(a),2(b) and 2(c) in the case of the circular Hough transform.
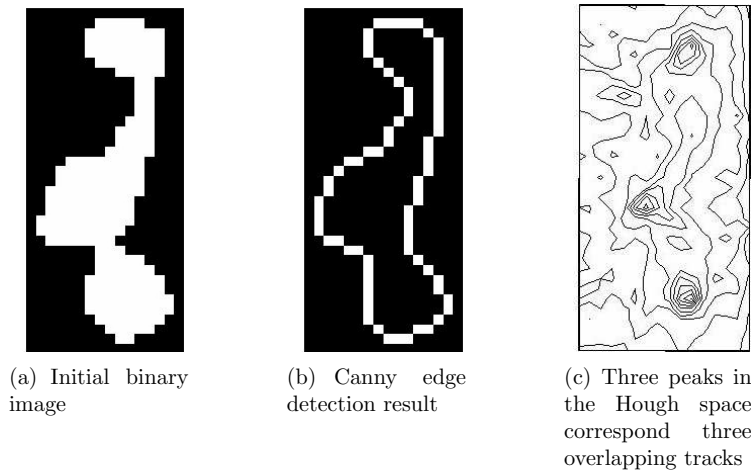

(a) Initial binary image

(b) Canny edge detection result

(c) Three peaks in the Hough space correspond three overlapping tracks

Figure 2. The recognition of three overlapped tracks using the Hough transform.

3. Uses of TRIAC II code

3.1. Radon's progeny behavior

Using the first mode of TRIACII program and the CR-39 SSNT detector the distribution of the tracks created on the detector's surface from Radon and its progenies' alpha decay has been studied. A number of typical closed-type cylindrical shape Radon chamber were used. A thin polyethylene foil was used as a filter in order to prevent all other atoms except from Radon to diffuse in the chamber volume.Plates from CR39 SSNTD were placed towards the x(diameter)axis and z(height) axis of the cylindrical chamber as it is shown in Figure3. Different size chambers were exposed in a Radon rich environment

Figure 3. A typical Radon chamber closed-type.
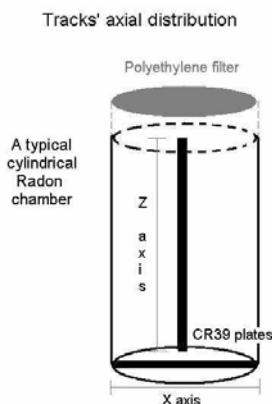
for a week. A typical chemical etching followed and a number of images were taken from the detectors' surfaces.All the regions of the detectors were "scanned" with a step of one millimeter. The results showed an uniform distribution of number of the tracks toward the x-axis but a decreasing one toward the z-axis. Closer to the upper side of the detectors the concentrations of the tracks were bigger for all the chambers. In the Figures 4(a) and 4(b) characteristic results are shown for a cylindrical detector with dimensions (x-z) 46mm-60mm.

3.2. Alpha-particles tracks' characteristics

One of the challenges, which attracted significant attention in the past is a formal description of the tracks' growth during the chemical etching procedure. The geometry of the track development has been considered by a number of authors[9]-[19]. Generally, the shapes of the tracks are elliptical and the parameters of the minor and the major axis depend on the energy and the incident angle of the particles. Also the shapes of the tracks are strongly dependent on etching times of the detectors. As the duration of chemical etching increases, the thickness of the removed layer and the openings of the tracks also increase. Moreover, the dependence of the tracks' axis's lengths on the energy of alpha particles is not linearly correlated with the thickness of the removed layers according to theoretical models [10], [13], [18], and [19]. Using an Am-241 source and foils of several

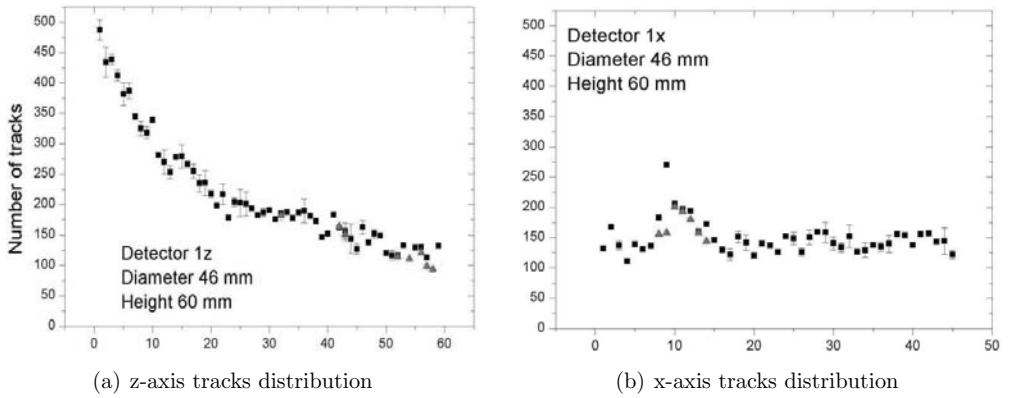(a) z-axis tracks distribution

(b) x-axis tracks distribution

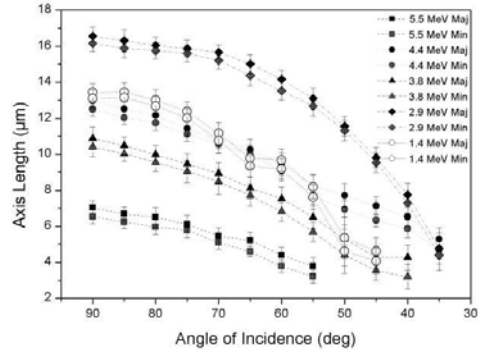Figure 4. Axial tracks' distribution inside a closed Radon chamber.

materials as absorbers, CR39 plates were exposed to four beams of different alpha particle energies inside a vacuum chamber in a range of angles 90°-35°. Using TRIACII program the parameters of major and minor axis and the brightness of the tracks have been estimated.The results are shown in Figures5(a),5(b),5(c) and 5(d)

The not linear correlation between the three main tracks' parameters has been experimentally verified for a several different chemical etching times (6 to 10 hours).

(a) Major axis vs Energy

(b) Minor axis vs Energy
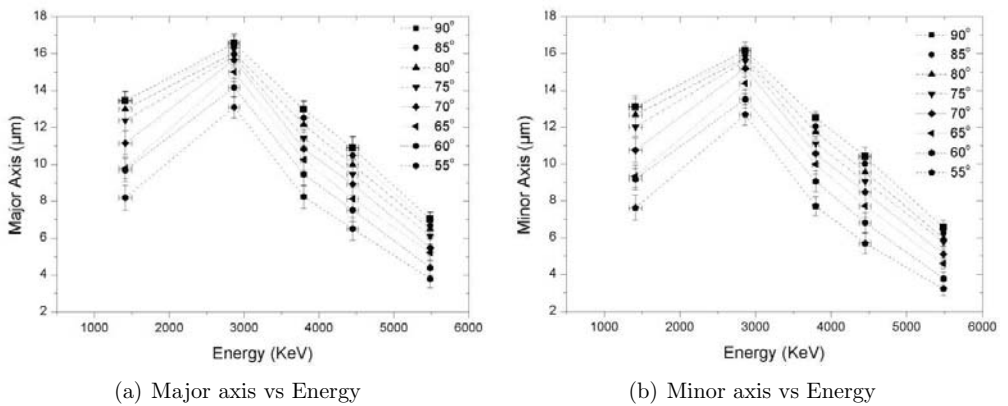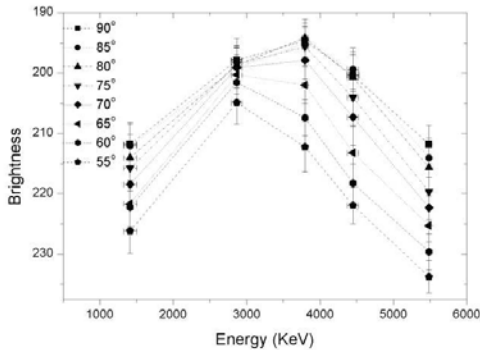
(c) Brightness axis vs Energy (d) Axis vs Angle of incidence

Figure 5. Tracks parameters for a standard 8h CE (the lines are only guides for the eye).

4. Conclusions

The computer code described here provides reproducible results at a scanning time of less than 3 minutes per image analyzed. It is easy to operate and when used in a systematic way provides reliable counting results, even when overlapping tracks exist.

REFERENCES

1. United Nation Scientific Committee on the Effects of Atomic Radiation. The Report to the General Assembly with scientific Annexes. New York: United Nations 2000
2. D. Nikezic, K. N. Yu, Materials Science and Engineering R46 (2004) 51-123
3. D. L. Patiris, K. Blekas, K. G. Ioannides, Nucl. Instrum. Methods Phys. Res. B 244 (2006) 392-396
4. N. K. Pal, S. K. Pal., Pattern Recognition 26 (1993) 1277
5. R .O. Duda, P. E. Hart, D. G. Stork, Pattern Classification. Wiley-Interscience, New York, 2001.
6. J. Canny, IEEE Transactions on Pattern Analysis and Machine Intelligence 8 (1986) 679
7. J. R. Parker. Algorithms for Image Processing and Computer Vision, New York, John Wiley and Sons, Inc., 1997
8. R. K. K. Yip, P. K. S. Tam, and D. N. K. Leung. "Modification of Hough transform for circles and ellipses detection using a 2-dimensional array", Pattern Recognition, (1992), vol. 25, 1007-1022
9. P. R. Henke, E. Benton, Nucl. Instrum. Methods 97 (1971) 483
10. G. Somogyi, A .S. Szalay, Nucl. Instrum. Methods 109 (1973) 211
11. G. H. Paretzke, E. Benton, P. R. Henke, Nucl. Instrum. Methods 108 (1973) 73
12. G. Somogyi, Nucl. Instrum. Methods 173 (1980) 21
13. M. Fromm, P. Meyer, A. Chambaudet, Nucl. Instrum. Methods Phys. Res. B 107

(1996) 337

14. R. Barillon, M. Fromm, A. Chambaudet, H. Marah, A. Sabir, Radiat. Meas. 28 (1997) 619
15. V. Ditlov, Radiat. Meas. 25 (1995) 89
16. D. Nikezic, D. Kostic, Radiat. Meas. 28 (1997) 185
17. D. Nikezic, Radiat. Meas. 32 (2000) 277
18. D. Nikezic, K. N. Yu, Radiat. Meas. 37 (2003) 39
19. A. P. Fews, D. L. Henshaw, Nucl. Instrum. Methods 197 (1982) 517